Synthesis of $CoCrFeO_4$ Nanoparticles Using Microemulsion Methods and Size-Dependent Studies of Their Magnetic Properties

Christy R. Vestal and Z. John Zhang*

School of Chemistry and Biochemistry, Georgia Institute of Technology, Atlanta, Georgia 30332-0400

Received February 5, 2002. Revised Manuscript Received June 13, 2002

Normal and reverse micelle microemulsion methods were used to synthesis single-phase $CoCrFeO_4$ nanoparticles with a controlled size range of 6−16 nm and a size distribution of 14%. The size-dependent magnetic properties were characterized and found to agree well with Stoner−Wohlfarth theory. The results from nanoparticles prepared by the normal micelle and reverse micelle microemulsion methods were consistent with each other. The $CoCrFeO_4$ nanoparticles did not display the types of anomalous magnetic properties reported for their bulk-phase material. Using $CoCrFeO_4$ nanoparticles as precursors for the formation of a bulk sample resulted in a material that displayed an unusual susceptibility behavior but not the anomalous temperature-dependent hysteresis trend usually observed in conventional $CoCrFeO_4$ bulk materials.

Introduction

Nanometer-scale materials have generated considerable interest because of their unique relationship between size and physical properties.[1] Superparamagnetism is an interesting phenomenon that occurs usually in magnetic nanoparticles.[2,3] Understanding and controlling this behavior is critically important in the technological applications of magnetic nanoparticles such as data storage,[4] magnetocaloric refrigeration,[5] drug delivery,[6] and magnetic resonance imaging (MRI) contrast enhancement.[7] From a fundamental standpoint, magnetic nanoparticles below a critical diameter exhibit a single-domain magnetic structure that might provide insight into the quantum origins of magnetism arising from magnetic couplings at the atomic level such as the coupling between the spin of the electron and quantum momentum of its atomic orbital (L−S coupling).

Spinel ferrite MFe_2O_4 (M = Mn, Co, Ni, Zn, etc.) nanoparticles are an ideal system for investigating the relationship between the magnetic properties and crystal chemistry of materials.[8] A type of interesting nanoparticle for the investigation of the changes in magnetization in a single-domain magnetic structure is the mixed spinel ferrite $CoCrFeO_4$ in which Fe is partially replaced by Cr. Because Cr has a weaker magnetic moment than Fe, this partial replacement of elements might cause magnetic frustration. The bulk magnetic properties have been reported to be anomalous as a result of a frustrated magnetic structure.[9] Examples of the anomalous behavior include sharp decreases in the saturation magnetization versus temperature curve at ∼100 and 330 K. Also, a cusp in the susceptibility curve is usually observed at 330 K, just before the reported Curie transition temperature, T_C, of $CoCrFeO_4$.[9,10] The decrease at ∼100 K is believed to be a result of a transition from a sperimagnetic phase (a frustrated structure) into a cluster spin glass. The anomaly at 330 K is a transition from the cluster spin glass to a paramagnetic state. To further complicate the issues, a wide variety of Curie temperatures of 330−360, 475, and 780 K have also been reported.[9−11]

$CoCrFeO_4$ nanoparticles should have a single-domain magnetic structure, which might offer a simpler system for understanding the magnetic behavior of $CoCrFeO_4$ materials. Xiong et al. recently reported the synthesis and magnetic characterization of $CoCrFeO_4$ nanoparticles with a size of 8.1 nm by using a sol−gel method.[11] However, the size dependence of magnetic properties and issues relating to the anomalous behavior remain untouched. Although a variety of spinel ferrite nanoparticles have been synthesized by various methods,[12−17] microemulsion methods provide a synthetic approach

* To whom correspondence should be addressed.

(1) Service, R. F. *Science* **1996**, *271*, 920.
(2) Awschalom, D. D.; DiVencenzo, D. P. *Phys. Today* **1995**, *48* (4), 43.
(3) Aharoni, A. *Introduction to the Theory of Ferromagnetism*; Oxford University Press: New York, 1996; p 92.
(4) Sun, S.; Murray, C. B.; Weller, D.; Folks, L.; Moser, A. *Science* **2000**, *287*, 1989.
(5) McMichael, R. D.; Shull, R. D.; Swaertzendruber, L. J.; Bennett, L. H. *J. Magn. Magn. Mater.* **1992**, *111*, 29.
(6) *Scientific and Clinical Applications of Magnetic Carriers*; Häfeli, U., Schütt, W., Teller, J., Zborowski, M., Eds.; Plenum Press: New York, 1997.
(7) Mitchell, D. G. *J. Magn. Reson. Imaging* **1997**, *7*, 1.
(8) Liu, C.; Zou, B.; Rondinone, A. J.; Zhang, Z. J. *J. Am. Chem. Soc.* **2000**, *122*, 6263.
(9) Belov, K. P.; Goryaga, A. N.; Annaev, R. R.; Kokorev, A. I.; Lyamzin, A. N. *Sov. Phys. Solid State* **1989**, *31*, 785.
(10) Mohan, H.; Shaikh, I. A.; Kulkarni, R. G. *Physica B* **1996**, *217*, 292.
(11) Xiong, G.; Mai, Z.; Xu, M.; Cui, S.; Ni, Y.; Zhao, Z.; Wang, X.; Lu, L. *Chem. Mater.* **2001**, *13*, 1943.
(12) Moumen, N.; Pileni, M. P. *Chem. Mater.* **1996**, *8*, 1128.
(13) Pileni, M. P.; Moumen, N. *J. Phys. Chem. B* **1996**, *100*, 1867.

10.1021/cm020112k CCC: $22.00
Published on Web 07/30/2002

that allows for high-quality nanoparticles with a narrow size distribution to be made. Furthermore, by minor adjustments to the synthesis conditions, this approach easily allows for the size of nanoparticles to be controlled by means other than thermal annealing of the nanoparticles at various temperatures.[17,18] Variable-temperature annealing of samples not only changes the size of the nanoparticles but also might result in different cation redistributions depending on the annealing temperature.[19] The spinel structure contains two cation sites in the lattice: the A sites have a tetrahedral coordination by oxygen, and the B sites have an octahedral coordination. The magnetic properties of spinel ferrites are closely related to the magnetic couplings between the magnetic cations at the A and B sites. They are affected by the redistribution of cations between these two sites. Therefore, a direct correlation between magnetic properties and the size of spinel ferrite nanoparticles is not straightforward when variable-temperature annealing is used to control the size variation.

Herein, we report the use of microemulsion methods to synthesize $CoCrFeO_4$ nanoparticles with controlled sizes ranging from 6 to 16 nm and a size distribution of 14%. Their corresponding magnetic properties as a function of size have also been studied. The $CoCrFeO_4$ nanoparticles did not display the types of anomalous magnetic properties reported for their bulk material.

Experimental Section

Nanoparticle Synthesis. Both normal and reverse micelle microemulsion methods were used to synthesize $CoCrFeO_4$ spinel ferrite nanoparticles. Aqueous solutions containing $CoCl_2 \cdot 6H_2O$ (Fisher, 98%), $CrCl_3 \cdot 6H_2O$ (Aldrich, >98%), and $Fe(NO_3)_3 \cdot 9H_2O$ (Alfa Aesar, >98%) were mixed in an equimolar ratio. To form the normal micelles, an aqueous solution of sodium dodecyl sulfate (Aldrich, 98%) was added to the cation mixture and stirred constantly. A dark slurry was formed after the addition of methylamine (Acros, 40% in water). Following the chemometric model developed by Rondinone et al., the size of the $CoCrFeO_4$ nanoparticles was controlled by adjusting the temperature at which the mixture was heated and stirred over the next several hours.[18] To form the reverse micelles, an aqueous solution of sodium dodecylbenzenesulfonate (Aldrich, 98%) was added to the equimolar cation solution, followed by a large volume of toluene (J.T. Baker, ACS-grade). The solution was stirred overnight to complete the formation of reverse micelles. Methylamine was added to precipitate the nanoparticles, followed by refluxing the solution for several hours. Varying the water-to-toluene ratio controlled the size of the nanoparticles. In both microemulsion procedures, the samples were washed with ethanol and water to remove excess surfactant. Then, the nanoparticles were collected by centrifugation. The samples were heated to 600 °C in air for 20 h to form crystalline nanoparticles.

X-ray Diffraction. X-ray diffraction data were collected with a Bruker D8 ADVANCE X-ray diffractometer using Cu Kα radiation. Particle sizes were determined from the average peak broadening of the five strongest diffraction peaks by using the commercial program TOPAS.

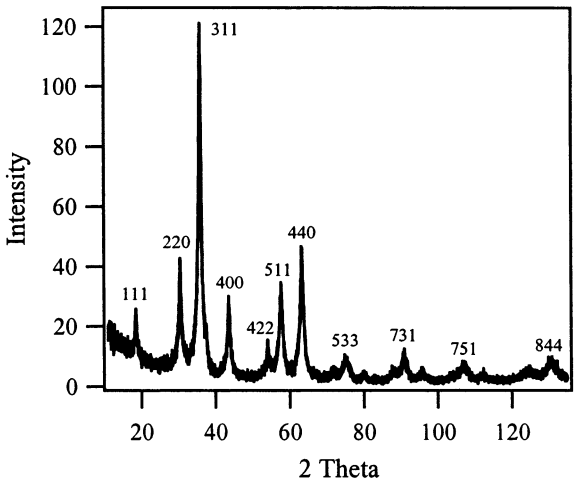

Figure 1. X-ray diffraction pattern of 11-nm $CoCrFeO_4$ nanoparticles.

Transmission Electron Microscopy. Transmission electron microscopy (TEM) studies were performed using a JEOL 100C instrument operating at 100 kV. Nanoparticles were dispersed onto a holey carbon grid. Particle size distributions were determined by manually counting over 100 particles.

Magnetic Measurements. Magnetic measurements were performed with a Quantum Design MPMS-5 SQUID magnetometer. Zero-field-cooled (ZFC) susceptibility measurements were conducted by cooling the sample from room temperature to 5 K under no applied field. Then, a field of 100 G was applied, and the change in magnetization was recorded as the nanoparticles were slowly warmed. Field-cooled (FC) susceptibility experiments were performed by applying a 100-G field before cooling the sample to 5 K. Hysteresis measurements were carried out at 5 and 300 K in applied fields up to 5 T. In the low-temperature hysteresis measurements, the nanoparticles were mixed with eicosane ($C_{20}H_{42}$, Aldrich) to prevent physical shifting of the nanoparticles.

Results and Discussion

Nanoparticle Synthesis and Size-Dependent Characterization. Both normal and reverse micelle microemulsion methods produced $CoCrFeO_4$ nanoparticles consisting of a pure spinel phase, as indicated by the results of the X-ray diffraction studies (Figure 1). Average particle sizes were determined from the broadening of X-ray diffraction peaks using the Scherrer equation and found to range from 8 to 16 nm when the normal micelle method was employed and from 6 to 11 nm when the reverse micelle method was used. Particle sizes were confirmed using TEM (Figure 2) and the size distribution was ~14% (Figure 3). Advantages of using the reverse micelle method include being able to form smaller particles and also relatively easier control of the size of the nanoparticles. However, the reverse micelle synthesis involves the handling and disposal of large quantities of organic wastes. The normal micelle method allows for easier formation of larger nanoparticles and a "green" cleanup. In terms of the properties of the nanoparticles such as size distribution, these two methods generated similar results. Elemental analysis by inductively coupled plasma atomic emission spectroscopy (ICP-AES) confirmed an equimolar ratio of metal cations in the nanoparticles and provided a chemical composition of $CoFe_{1.01\pm.03}Cr_{1.00\pm.03}O_4$.

(14) Perez, J. A. L.; Quintela, M. A. L.; Mira, J.; Rivas, J.; Charles, S. W. *J. Phys. Chem. B* **1997**, *101*, 8045.
(15) Chen, Q.; Zhang, Z. J. *Appl. Phys. Lett.* **1998**, *73*, 3156.
(16) Chen, Q.; Rondinone, A. J.; Chakoumakos, B. C.; Zhang, Z. J. *J. Magn. Magn. Mater.* **1999**, *194*, 1.
(17) Liu, C.; Zou, B.; Rondinone, A. J.; Zhang, Z. J. *J. Phys. Chem. B* **2000**, *104*, 1141.
(18) Rondinone, A. J.; Samia, A. C. S.; Zhang, Z. J. *J. Phys. Chem. B* **2000**, *104*, 7919.
(19) Zhang, Z. J.; Wang, Z. L.; Chakoumakos, B. C.; Yin, J. S. *J. Am. Chem. Soc.* **1998**, *120*, 1800.

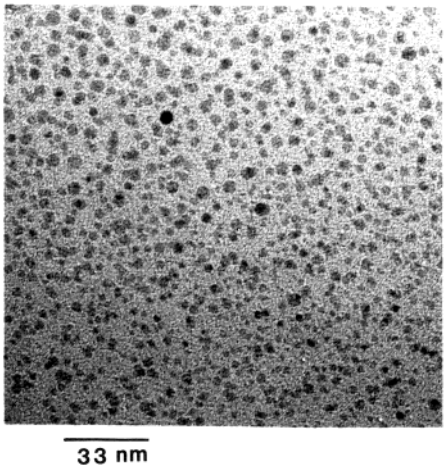

Figure 2. TEM micrograph of $CoCrFeO_4$ nanoparticles with an average size of ~6 nm.

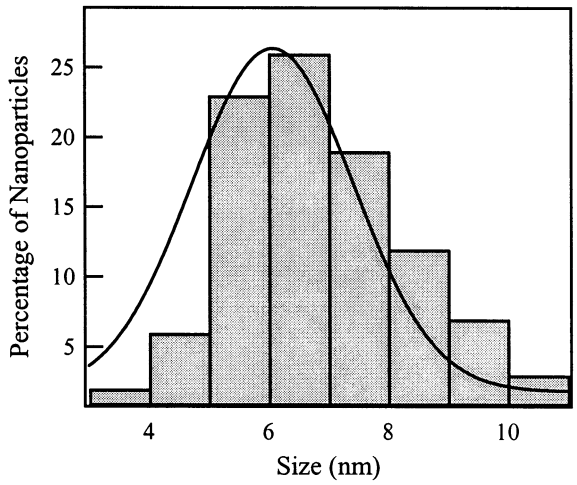

Figure 3. TEM size distribution histogram with a size distribution of ~14%.

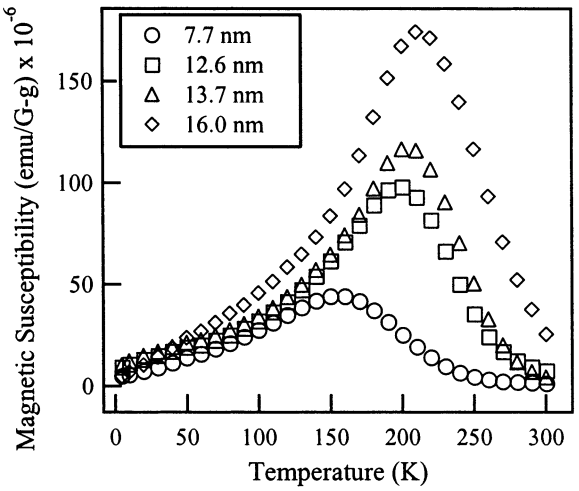

Figure 4. Temperature dependence of ZFC susceptibility for $CoCrFeO_4$ nanoparticles of various sizes under a magnetic field of 100 G.

The temperature-dependent ZFC measurement of magnetic susceptibility for $CoCrFeO_4$ nanoparticles with varying sizes is shown in Figure 4. For all samples, the magnetic susceptibility initially increases as temperature increases and at a certain temperature reaches a maximum. This maximum point is referred to as the blocking temperature, T_B. At temperatures above the blocking temperature, the magnetization decreases, and the nanoparticles display paramagnetic behavior. Figure 5 shows the increase in blocking temperature as the size of the nanoparticles increases and also the good agreement between the results for the particles synthesized by the reverse micelle method and by the normal micelle method.

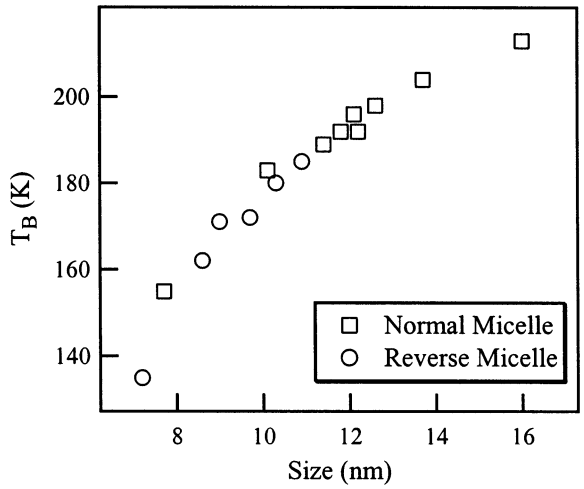

Figure 5. Size dependence of blocking temperature under a 100-G field for nanoparticles prepared by the normal and reverse micelle procedures.

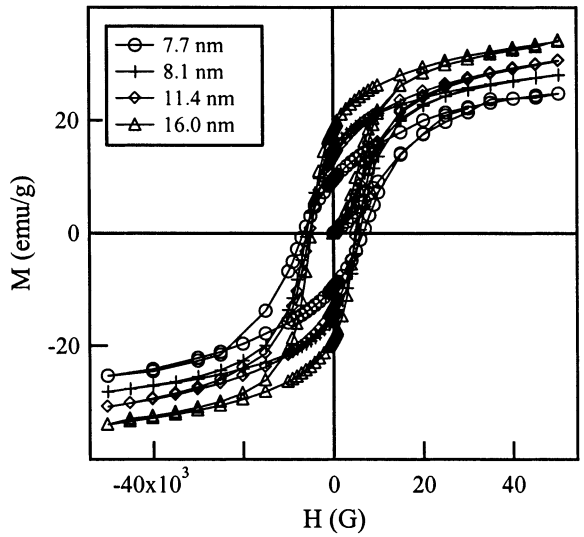

Figure 6. Field-dependent magnetization of $CoCrFeO_4$ nanoparticles with various sizes at 5 K.

At temperatures below the blocking temperature, the field-dependent magnetization of the $CoCrFeO_4$ nanoparticles displays hysteresis. Figure 6 shows the hysteresis curves at 5 K for $CoCrFeO_4$ nanoparticles with different sizes. The remnant magnetization (M_R) clearly increases as the size increases, as shown in Figure 7a. Furthermore, there is good agreement between the results for the samples synthesized by the two microemulsion methods. Although there is a bit more scatter in the saturation magnetization (M_S) and coercivity (H_C) trends, it is clear that the saturation magnetization increases as a function of size while the coercivity decreases (Figure 7b,c). In all samples, the hysteresis disappears at temperatures above the blocking temperature.

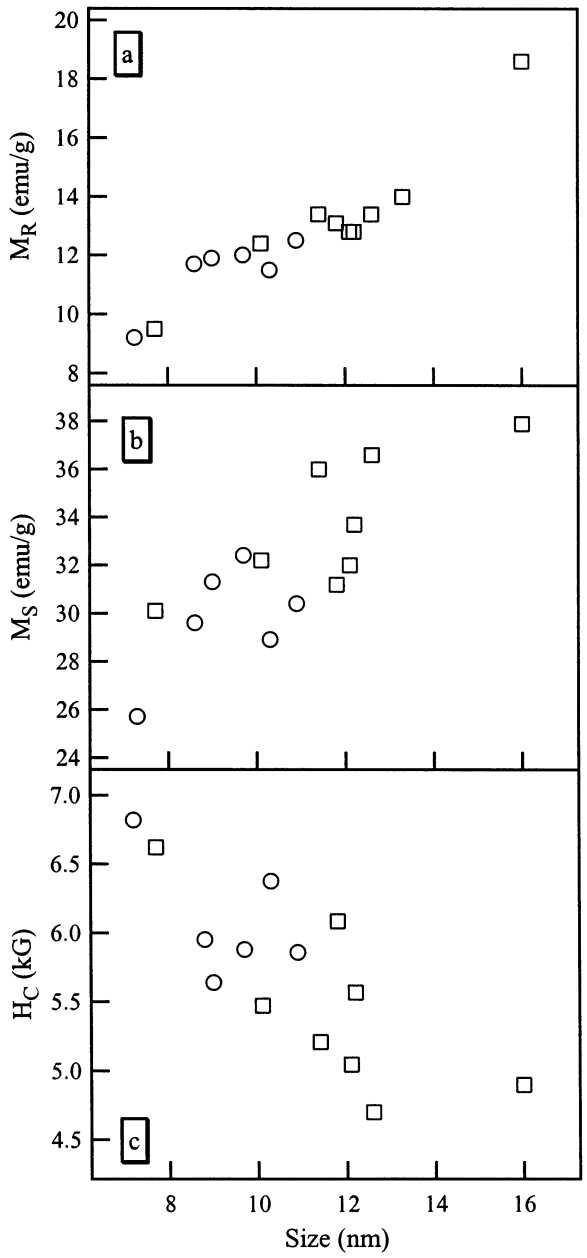

Figure 7. (a) Size dependence of remnant magnetization for $CoCrFeO_4$ nanoparticles. (b) Size dependence of saturation magnetization. (c) Size dependence of coercivity. The open circles (○) represent nanoparticles prepared by the reverse micelle procedure, and the open squares (□) represent nanoparticles synthesized by the normal micelle procedure.

The size-dependent relationship of the blocking temperature (Figure 5) is consistent with the size dependence of the magnetocrystalline anisotropy energy (E_A). According to Stoner−Wohlfarth theory, the E_A of a single-domain particle is given by

$$E_A = KV \sin^2 \theta \qquad (1)$$

where K is the anisotropy energy constant and reflects the strength of the L−S couplings, V is the volume of the nanoparticle, and θ is the angle between the applied magnetic field and the easy axis of the nanoparticles.[20] Below a critical size, the magnetocrystalline anisotropy energy becomes comparable with the thermal activation energy, k_BT, where k_B is the Boltzmann constant, and the magnetization direction of the nanoparticle can easily be moved away from its easy axis by thermal activation. T_B represents the point at which thermal activation is strong enough to overcome the anisotropy energy, E_A. Because E_A increases with increasing size of the nanoparticles, more energy is needed to overcome this increasing energy barrier, and hence, the threshold point (T_B) of thermal activation increases with nanoparticle size (Figure 5).

A blocking temperature of 249 K in a 100-G field was reported by Xiong et al. for their 8.1-nm $CoCrFeO_4$ nanoparticles synthesized by the sol−gel method.[11] This temperature is ∼90 K above that of our similarly sized nanoparticles. Although the exact reasons for this discrepancy are not clear, it is well-known that particles produced by different synthesis routes might exhibit different magnetic and structural properties for a variety of reasons including whether kinetic or thermodynamic control affects the cation distribution in the chosen synthesis route.[21] In addition, postsynthesis annealing might also change the cation distribution, and hence, affect the magnetic results.[19] In the current case, 600 °C was used to anneal our nanoparticles, whereas Xiong et al. annealed their samples at 500 °C.

The cation distributions cannot be determined in $CoCrFeO_4$ materials by conventional X-ray diffractometry because of the similar values of the X-ray scattering factor for the metal cations. We approximated our cation distribution from SQUID susceptibility measurements using eq 2

$$\chi = \sigma_s \mu/(3k_BT) \qquad (2)$$

where σ_s is the saturation magnetization and μ is the magnetic moment.[22] It was assumed that all Cr^{3+} ions occupied octahedral sites as reported for chromium-containing spinel ferrites,[23] and also that the distribution followed Néel's two-sublattice model for ferrimagnetism. Using the above conditions, the distribution was approximated to be $(Co_{0.42}Fe_{0.58})[Co_{0.57}Fe_{0.43}Cr]O_4$ where the cations in parentheses occupy A sites and the cations in brackets occupy B sites. This distribution is within the range that has been reported for the bulk system.[9,10] Because Xiong et al. did not provide information on the cation distribution of their nanoparticles, a direct comparison cannot be conducted. Because of strong couplings between chromium ions on the octahedral sites (J_{B-B}), Cr^{3+}-containing spinel ferrites often have canted magnetic spins, and deviations from Néel's model are common.[23] Clearly, a definite determination of the cation distribution can be very valuable in addressing the issue. Neutron diffraction studies on the cation distribution of these nanoparticles are currently planned in our laboratory.

The hysteresis behavior of the $CoCrFeO_4$ nanoparticles is also consistent with the temperature depen-

(20) Stoner, E. C.; Wohlfarth, E. P. *Philos. Trans. R. Soc. A* **1948**, *240*, 599; reprinted in *IEEE Trans. Magn.* **1991**, *27*, 3475.

(21) Pandya, P. B.; Joshi, H. H.; Kulkarni, R. G. *J. Mater. Sci. Lett.* **1991**, *10*, 474.

(22) Chen, J. P.; Sorenson, C. M.; Klabunde, K. J.; Hadjipanayis, G. C. *Phys. Rev. B* **1995**, *51*, 11527.

(23) Van Groenou, B. A.; Bongers, P. F.; Stuyts, A. L. *Mater. Sci. Eng.* **1968/69**, *3*, 317.

dence of the magnetocrystalline anisotropy energy. Because the magnetocrystalline anisotropy is overcome at temperatures above the blocking temperature, the nanoparticle magnetization direction changes concurrently with the direction of applied field. As a result, the hysteresis disappears. The size-dependent trends for the field-dependent magnetization agree well with Stoner−Wohlfarth theory for the coercivity H_C of a single-domain nanoparticle, which is represented by

$$H_C = 2K/(\mu_o M_S) \quad (3)$$

where μ_o is a universal constant of permeability in free space and M_S is the saturation magnetization of the nanoparticle.[24] Figure 7b shows that the saturation magnetization of the $CoCrFeO_4$ nanoparticles increases as the size increases. From the inverse relationship between saturation magnetization and coercivity (eq 3), assuming that the magnetocrystalline anisotropy remains constant, it is expected the coercivity should decrease as size increases. This trend is indeed observed in Figure 7c. Certainly, it is highly questionable that the anisotropy constant K would remain unchanged as the size of the nanoparticles changes. However, as long as the K value does not change drastically, the trend should still be consistent with the prediction of Stoner−Wohlfarth theory.

Studies of Nanoparticles with Regard to Anomalous Bulk Properties. The field-dependent magnetization of $CoCrFeO_4$ nanoparticles with a size of ∼10 nm was measured over a temperature range of 5−180 K (the blocking temperature for these nanoparticles was 180 K). Figure 8a shows the saturation magnetization decreasing smoothly with increasing temperature. The more rapid decrease at very low temperature suggests that Bloch's $T^{3/2}$ law is not followed, which is commonly observed in nanoparticulate magnetic systems. High-temperature susceptibility measurements indicate that the Curie temperature of these nanoparticles is ∼780 K.

A bulk sample was prepared by heating the ∼10-nm $CoCrFeO_4$ nanoparticles at 1100 °C for 48 h. Sharp X-ray diffraction peaks confirm that the crystal grain size has grown and that a bulk phase has been formed. The field-dependent magnetization of this bulk sample was measured from 5 to 400 K. Figure 8b shows that the saturation magnetization changes very little initially when the temperature is raised but then decreases almost linearly. High-temperature susceptibility measurements indicate that the Curie temperature remains at ∼780 K in the bulk sample. However, a peak at ∼287 K occurs in the low-temperature susceptibility curve for the bulk sample. This temperature does not correspond to the T_B of 180 K in the precursor nanoparticles.

Previous studies on the magnetic properties of bulk $CoCrFeO_4$ materials have reported some interesting but complex anomalous magnetic properties. The most distinctive features include a cusp in the susceptibility measurements at ∼330 K, just before the reported Curie transition temperature of 358 K. Also, the saturation magnetization versus temperature curve usually shows sharp decreases at 100 K and at this cusp temperature

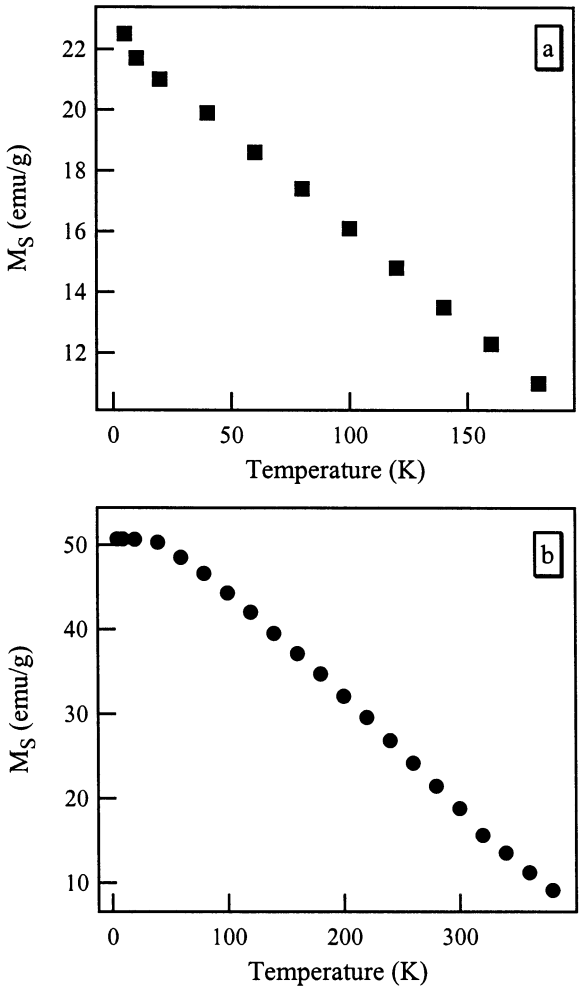

Figure 8. Saturation magnetization as a function of temperature for (a) ∼10-nm $CoCrFeO_4$ nanoparticles and (b) bulk-phase sample prepared from the ∼10-nm nanoparticulate precursors.

of ∼330 K.[9,10] It was reasoned that these anomalous properties are due to the magnetic transitions related to the frustrated structure in the $CoCrFeO_4$ material. In some types of frustrated magnetic structures, spontaneously separated regions exist, and each region has its own distinct magnetic phase. Magnetic ordering does not go through the whole sample space. Sperimagnetic materials exhibit one type of frustrated structure in which the isolated regions display ferrimagnetic ordering. $CoCrFeO_4$ bulk materials have been considered to have the sperimagnetic structure. $CoCrFeO_4$ contains three different magnetic cations, and therefore, various combinations of magnetic exchange interaction between lattice sites can occur. The magnitude of magnetic exchange interactions can vary greatly. For instance, the exchange coupling between Cr^{3+} cations at B lattice sites has a large negative exchange constant J_{B-B}. Moreover, different magnetic cations also exhibit different anisotropy strengths. Co^{2+} usually acts as a highly anisotropic ion. Because of the presence of such metal cations with different anisotropic strengths and very diverse exchange couplings, different magnetic states might exist in mixed spinel ferrite $CoCrFeO_4$ and result in a frustrated magnetic structure.[25,26] The

(24) McCurrie, R. A. *Ferromagnetic Materials—Structure and Properties*; Academic Press: London, 1994; p 16.

(25) Shellmyer, D. J.; Nafis, S. *J. Appl. Phys.* **1985**, *57*, 3584.

anomalous properties have been considered to be indications of such a frustrated structure. The transition at ~100 K was reported to be the result of a magnetic transition from a sperimagnetic phase into a cluster spin glass. The anomaly around 330 K was believed to be a transition between the cluster spin glass and a paramagnetic state.

Interestingly, none of these anomalous properties are observed in $CoCrFeO_4$ nanoparticles. It is highly likely that the limited size and also the single-magnetic-domain nature of magnetic nanoparticles severely restrict the formation of isolated regions with different magnetic orderings as observed in typical frustrated materials. Because of the lack of observable anomalous properties, the magnetic moments in $CoCrFeO_4$ nanoparticles probably do not order into a frustrated structure.

It is very intriguing that the $CoCrFeO_4$ sample with a bulk phase prepared from $CoCrFeO_4$ nanoparticles also did not display the same anomalous properties as reported for the bulk materials made by ceramic routes. Unlike the ceramic bulk materials that displayed a sharp decrease of saturation magnetization at 100 and 330 K, the saturation magnetization versus temperature trend decreases smoothly in our bulk material (Figure 8b). A peak at 287 K in the low-temperature susceptibility measurement was found, and we cannot explain such a transition without input from neutron diffraction studies. However, no consequence of this transition can be observed around this temperature in the temperature-dependent saturation magnetization trend. At the current stage, we do not know why bulk materials from a single-domain nanoparticulate precursor avoid the anomalous behavior that is usually seen in bulk samples prepared by conventional ceramic routes. We speculate that this might be the consequence of a lack of frustrated structure in the precursor nanoparticles. When the nanoparticles were heated at 1100 °C, the crystal grains grew slowly, and the magnetic structure was always at a thermodynamic equilibrium. Therefore, any kinetic trapping of magnetic phases was prevented. Certainly, further studies are needed to determine the magnetic structure in the bulk-phase samples made from nanoparticulate precursors, and to elucidate the evolution of the magnetic structure from single-domain nanoparticles to bulk-phase materials.

(26) Chudnovsky, E. M. *J. Appl. Phys.* **1988**, *64*, 5770.

Conclusion

Microemulsion methods were used to synthesize single-phase $CoCrFeO_4$ nanoparticles over a size range of 6−16 nm. The size-dependent magnetic properties were characterized and found to agree well with Stoner−Wohlfarth theory. The $CoCrFeO_4$ nanoparticles did not display the types of anomalous magnetic properties reported for bulk $CoCrFeO_4$ materials. Using our nanoparticles as precursors for a bulk sample resulted in a material that displayed an unusual susceptibility behavior but not an anomalous trend in saturation magnetization versus temperature. Single-magnetic-domain precursors clearly affect the magnetization processes in the bulk materials produced. Using nanoparticulate precursors might offer a route for reducing the frustration in magnetic materials or provide an alternate route for adjusting the magnetic ordering of bulk materials.

Acknowledgment. C.R.V. is partially supported by a Molecular Design Institute Fellowship. This research is supported in part by the NSF (DMR-9875892), the Beckman Young Investigator program of the Arnold & Mabel Beckman Foundation, Sandia National Laboratory, and the PECASE Program. TEM studies were carried out in the Electron Microscopy Center at Georgia Tech.

CM020112K